all imaged spinal cord sections to rule out possible axon intersections. Notably, in all of the collaterally sprouted axons from both mutant and wild-type animals, NG2$^+$ glial processes were barely detectable at the nodal vicinity (Fig. 4I), whereas many nonsprouted nodes appeared to be in contact with NG2$^+$ glial processes (Fig. 4J). This observation further indicates that nodal ensheathment is necessary to prevent axonal sprouting.

In conclusion, we find that isolated membranes of CNS nodes of Ranvier are nonpermissive for neurite outgrowth and propose that this is due to cell extensions that emanate from NG2$^+$ oligodendrocyte precursor-like cells that tightly ensheath the nodal axon. It is known that NG2 is expressed by a heterogeneous population of neuroglial cells in the adult CNS, ranging from oligodendrocyte precursors to specialized glial cells that contact nodes of Ranvier in optic nerves and synaptic terminals in the hippocampus (*29*–*31*). Whether these nodal glial cells represent the same lineage of specialized NG2$^+$ neuroglia described to contact nodes of Ranvier in rat optic nerves remains to be determined. Furthermore, we found glial processes emanating from specialized oligodendrocyte-like cells that converge at the CNS node and contain high concentrations of the neurite outgrowth inhibitor, OMgp. OMgp was detected at most of the nodes examined, which suggests that it may function in generating normal nodal architecture and in suppressing collateral sprouting, because in OMgp-null mice, the nodal gap is abnormally widened and sprouting from this locus is observed. It also remains to be determined whether OMgp is necessary for survival of the NG2$^+$ oligodendrocyte precursor-like cells, although given the lack of decrease in NG2$^+$ cells in the OMgp$^{-/-}$ mice, this may not be a likely functional role for OMgp. It seems more likely that OMgp plays a role in the adhesion of NG2$^+$ glial processes to CNS nodes because in all of the observed sprouted nodes, there were no detectable NG2$^+$ processes.

Finally, considering the intimate relation between the node and the encircling inhibitory glial membranes, after traumatic injury to the CNS, OMgp and possibly other inhibitory peptides at the nodal/paranodal region, such as versican, MAG, NG2, or Nogo-A (*11*, *16*, *27*, *32*), may remain stably attached to the nodal region or become deposited on the axonal surface, thus preventing axons from responding to injury-elicited growth signals. Overcoming the inhibitory nature of these nodal glial cells may yield new therapeutic interventions to promote functional recovery after CNS trauma.

References and Notes

1. L. Pedraza, J. K. Huang, D. R. Colman, *Neuron* **30**, 335 (2001).
2. J. R. Slack, W. G. Hopkins, M. N. Williams, *Nature* **282**, 506 (1979).
3. Q. T. Nguyen, J. R. Sanes, J. W. Lichtman, *Nat. Neurosci.* **5**, 861 (2002).
4. M. E. Schwab, P. Caroni, *J. Neurosci.* **8**, 2381 (1988).
5. G. R. Phillips *et al.*, *Neuron* **32**, 63 (2001).
6. W. T. Norton, S. E. Poduslo, *J. Neurochem.* **21**, 749 (1973).
7. S. Einheber *et al.*, *J. Cell Biol.* **139**, 1495 (1997).
8. M. Menegoz *et al.*, *Neuron* **19**, 319 (1997).
9. S. Tait *et al.*, *J. Cell Biol.* **150**, 657 (2000).
10. S. Lambert, J. Q. Davis, V. Bennett, *J. Neurosci.* **17**, 7025 (1997).
11. U. Bartsch, F. Kirchhoff, M. Schachner, *J. Comp. Neurol.* **284**, 451 (1989).
12. M. P. Washburn, D. Wolters, J. R. Yates III, *Nat. Biotechnol.* **19**, 242 (2001).
13. A. P. Goldsmith, S. J. Gossage, C. ffrench-Constant, *J. Neurosci. Res.* **78**, 647 (2004).
14. G. Mukhopadhyay, P. Doherty, F. S. Walsh, P. R. Crocker, M. T. Filbin, *Neuron* **13**, 757 (1994).
15. B. P. Niederost, D. R. Zimmermann, M. E. Schwab, C. E. Bandtlow, *J. Neurosci.* **19**, 8979 (1999).
16. T. Oohashi *et al.*, *Mol. Cell. Neurosci.* **19**, 43 (2002).
17. R. Sivasankaran *et al.*, *Nat. Neurosci.* **7**, 261 (2004).
18. V. Kottis *et al.*, *J. Neurochem.* **82**, 1566 (2002).
19. K. C. Wang *et al.*, *Nature* **417**, 941 (2002).
20. D. D. Mikol, K. Stefansson, *J. Cell Biol.* **106**, 1273 (1988).
21. C. Brunner, H. Lassmann, T. V. Waehneldt, J. M. Matthieu, C. Linington, *J. Neurochem.* **52**, 296 (1989).
22. A. Peters, S. Palay, H. Webster, *The Fine Structure of the Nervous System* (Oxford Univ. Press, New York, ed. 3, 1991).
23. R. H. Miller, B. P. Fulton, M. C. Raff, *Eur. J. Neurosci.* **1**, 172 (1989).
24. C. ffrench-Constant, R. H. Miller, J. Kruse, M. Schachner, M. C. Raff, *J. Cell Biol.* **102**, 844 (1986).
25. J. M. Levine, J. P. Card, *J. Neurosci.* **7**, 2711 (1987).
26. C. L. Dou, J. M. Levine, *J. Neurosci.* **14**, 7616 (1994).
27. A. M. Butt *et al.*, *Glia* **26**, 84 (1999).
28. D. Mikol *et al.*, *J. Cell Biol.* **111**, 2673 (1990).
29. D. E. Bergles, J. D. Roberts, P. Somogyi, C. E. Jahr, *Nature* **405**, 187 (2000).
30. M. Berry, P. Hubbard, A. M. Butt, *J. Neurocytol.* **31**, 457 (2002).
31. J. M. Levine, R. Reynolds, J. W. Fawcett, *Trends Neurosci.* **24**, 39 (2001).
32. D. Y. Nie *et al.*, *EMBO J.* **22**, 5666 (2003).

33. We thank D. Mikol, P. Brophy, and G. Gennarini for providing antibodies, and members of the D.R.C. lab for helpful suggestions. This work was supported by grants from the Canadian Institutes of Health Research and the NIH (NS20147), the National Multiple Sclerosis Society (RG 3217-A-8), the Myelin Repair Foundation, and the New York State Spinal Cord Injury Trust (NYS CO17683) to D.R.C. J.R.Y. was supported by NIH grant P41 RR11823.

Supporting Online Material
www.sciencemag.org/cgi/content/full/1118313/DC1
Materials and Methods
Movies S1 and S2

2 August 2005; accepted 4 November 2005
Published online 17 November 2005;
10.1126/science.1118313
Include this information when citing this paper.

The Widespread Impact of Mammalian MicroRNAs on mRNA Repression and Evolution

Kyle Kai-How Farh,[1]* Andrew Grimson,[1]* Calvin Jan,[1] Benjamin P. Lewis,[1,2] Wendy K. Johnston,[1] Lee P. Lim,[3] Christopher B. Burge,[2] David P. Bartel[1]†

Thousands of mammalian messenger RNAs are under selective pressure to maintain 7-nucleotide sites matching microRNAs (miRNAs). We found that these conserved targets are often highly expressed at developmental stages before miRNA expression and that their levels tend to fall as the miRNA that targets them begins to accumulate. Nonconserved sites, which outnumber the conserved sites 10 to 1, also mediate repression. As a consequence, genes preferentially expressed at the same time and place as a miRNA have evolved to selectively avoid sites matching the miRNA. This phenomenon of selective avoidance extends to thousands of genes and enables spatial and temporal specificities of miRNAs to be revealed by finding tissues and developmental stages in which messages with corresponding sites are expressed at lower levels.

MicroRNAs are an abundant class of endogenous ~22-nucleotide (nt) RNAs that specify posttranscriptional gene repression by base-pairing to the messages of protein-coding genes (*1*, *2*). Hundreds of miRNAs have been identified in humans (*1*), and thousands of messages are under selection to maintain pairing to miRNA seeds (nucleotides 2 to 7 of the miRNA), enabling regulatory targets of miRNAs to be predicted simply by searching 3′ untranslated regions (3′UTRs) for evolutionarily conserved 7-nt matches to miRNA seed regions (*3*–*5*).

We used the mouse expression atlas (*6*) to examine the expression of the predicted targets of six tissue-specific miRNAs: miR-1 and miR-133 (skeletal muscle), miR-9 and

[1]Whitehead Institute for Biomedical Research, Department of Biology, Massachusetts Institute of Technology, and Howard Hughes Medical Institute, 9 Cambridge Center, Cambridge, MA 02142, USA. [2]Department of Biology, Massachusetts Institute of Technology, Cambridge, MA 02139, USA. [3]Rosetta Inpharmatics, 401 Terry Avenue North, Seattle, WA 98109, USA.

*These authors contributed equally to this work.
†To whom correspondence should be addressed. E-mail: dbartel@wi.mit.edu

miR-124 (brain), miR-122 (liver), and miR-142-3p (hematopoietic organs and blood cells) (*7*–*10*) (fig. S1). The 250 messages with conserved miR-133 sites were generally expressed in muscle but at lower levels in muscle than in other tissues (Fig. 1A). Similarly, predicted targets of the other miRNAs were usually at lower levels in the tissue expressing the miRNA than in other tissues (Fig. 1A). Brain-specific miR-9 and miR-124 displayed more complex patterns, perhaps reflecting the heterogeneous cell types within the brain.

The low relative expression of predicted targets in differentiated tissues raised the question of whether they might be more highly expressed earlier in differentiation, before miRNA expression. To address this, we analyzed expression profiles of myotube differentiation (*11*), during which miR-1 and miR-133 accumulate after cell-cycle arrest (*12*). Predicted targets of these muscle-specific miRNAs were preferentially high before miRNA expression and then dropped as the miRNAs accumulated (Fig. 1B and fig. S3). Our observation that miRNAs induced during differentiation tend to target messages highly expressed in the previous developmental stage suggested a function analogous to that proposed for miRNAs in plants: They dampen the output of preexisting messages to facilitate a more rapid and robust transition to a new expression program (*13*). Predicted targets tended to be expressed at substantial levels on the absolute scale (Fig. 1A, *x* axis), which further suggested that metazoan miRNAs are often optimizing protein output without eliminating it entirely (*14*).

Our results are consistent with the idea that miRNAs are destabilizing many target messages to further define tissue-specific transcript profiles (*15*) but also leave open the possibility that many targets are repressed translationally without mRNA destabilization. If miRNAs were usually working in concert with transcriptional and other regulatory processes to down-regulate the same genes, then a correlation between conserved targeting and lower mRNA levels would be observed even for messages that miRNAs translationally repress without destabilizing.

Mammalian miRNA families have an average of ~200 conserved targets above estimated background, a figure approximately 1/10th the number of 3′UTRs with 7-nt sites in a single genome (*3*, *5*). Computational algorithms rely on evolutionary conservation to distinguish functional miRNA targets from the thousands of messages that would pair equally well; in contrast, the cell must rely on specificity determinants intrinsic to a single genome. To determine whether these nonconserved sites might be functional, we used reporter assays to compare repression mediated by conserved and nonconserved sites. We selected two targets of miR-1, predicted by TargetScan based on conservation in human, mouse, and rat (*16*) and six human UTRs that had comparable TargetScan scores in human but low or nonexistent scores in mouse or rat. When eight UTR fragments of ~0.5 kb that contained the sites were placed in reporters, we observed specific repression for all of them (Fig. 2A). Analogous experiments with eight predictions from our more sensitive analysis, TargetScanS, which searches for conserved 7- or 8-nt matches (*3*), and 17 genes with nonconserved matches also detected little difference between UTR fragments containing conserved and nonconserved sites (Fig. 2B), even when the concentration of transfected miRNA was titrated to suboptimal levels (fig. S4). Apparently, most nonconserved sites fortuitously reside in local contexts suitable for mediating repression and therefore have the potential to function when exposed to the miRNA. These results generalize previous work showing that in certain contexts 7- or 8-nt matches appear sufficient for miRNA-like regulation (*4*, *17*, *18*). We conclude that additional recognition features, such as pairing to the remainder of the miRNA, accessible mRNA structure, or protein-binding sites, are usually dispensable, or occur so frequently that they impart little overall specificity [supporting online material (SOM) text].

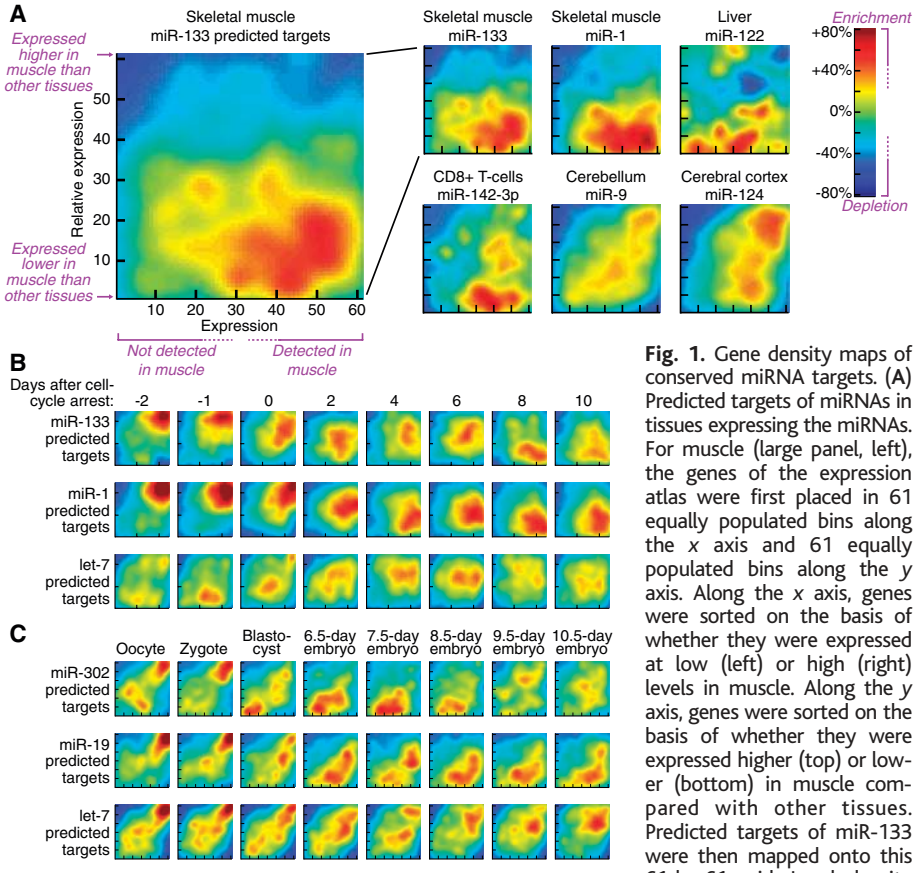

Fig. 1. Gene density maps of conserved miRNA targets. (**A**) Predicted targets of miRNAs in tissues expressing the miRNAs. For muscle (large panel, left), the genes of the expression atlas were first placed in 61 equally populated bins along the *x* axis and 61 equally populated bins along the *y* axis. Along the *x* axis, genes were sorted on the basis of whether they were expressed at low (left) or high (right) levels in muscle. Along the *y* axis, genes were sorted on the basis of whether they were expressed higher (top) or lower (bottom) in muscle compared with other tissues. Predicted targets of miR-133 were then mapped onto this 61-by-61 grid. Local density [after background subtraction (fig. S2) and smoothing] of miR-133 targets is color coded, with regions of enrichment (red) or depletion (blue) shown (key at far right). Other miRNA-tissue pairs were analyzed analogously (smaller panels, right). (**B**) Time course of predicted targets during myoblast (C2C12) differentiation to myotubes, analyzed with a 24-by-24 grid. (**C**) Time course of predicted targets during mouse embryogenesis, analyzed as in (A). Predicted targets of let-7 are included for comparison in (B) and (C).

To explore the impact of this vast potential for nonconserved targeting, we examined the expression of messages with nonconserved 7-nt matches to tissue-specific miRNAs, focusing first on messages with sites present in mouse but not in the orthologous human UTRs (Fig. 3A). In contrast to the conserved sites, the nonconserved sites had a propensity to fall in the UTRs of genes that were not expressed in the same tissue as the miRNA. Also notable was the depletion of sites among those genes that were most highly and specifically expressed in the tissue. Such depletion could result primarily from direct miRNA-mediated destabilization of messages (*15*), or some depletion might be from selective avoidance of sites—evolutionary pressure for messages highly specific to a tissue to lose sites for coexpressed miRNAs.

To distinguish between these two possibilities, we plotted the expression, in mouse,

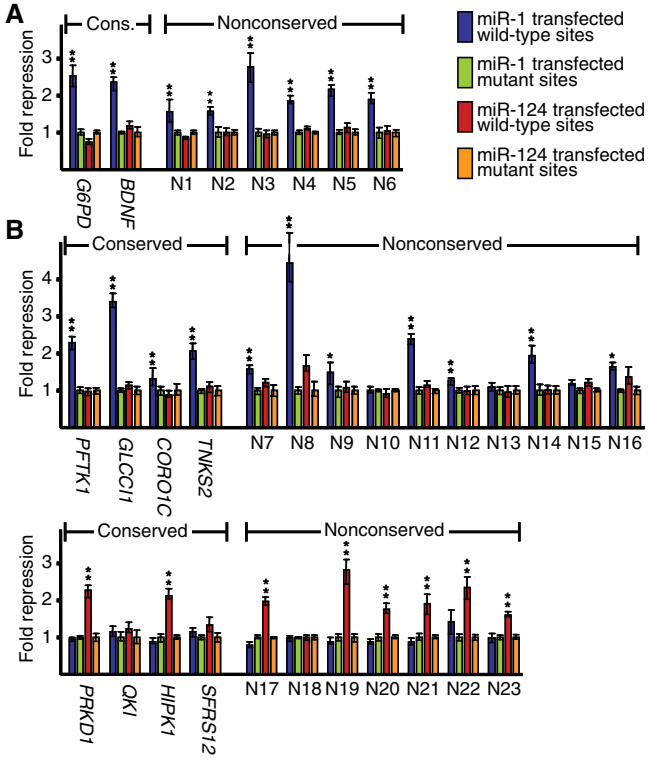

Fig. 2. MicroRNA-mediated repression of luciferase reporter genes containing 3′UTR fragments with conserved or nonconserved sites. (**A**) UTR fragments with TargetScan-like miR-1 sites. Luciferase activity from HeLa cells cotransfected with miRNA and wild-type reporters was normalized to that from cotransfection with mutant reporters with three point substitutions disrupting each seed match. The miR-124 transfections served as specificity controls. Error bars represent the third largest and smallest values among 12 replicates (one asterisk, $P < 0.01$; two asterisks, $P < 0.001$, Wilcoxon rank-sum test). (**B**) UTR fragments with TargetscanS-like miR-1 (top) and miR-124 (bottom) sites, analyzed as in (A).

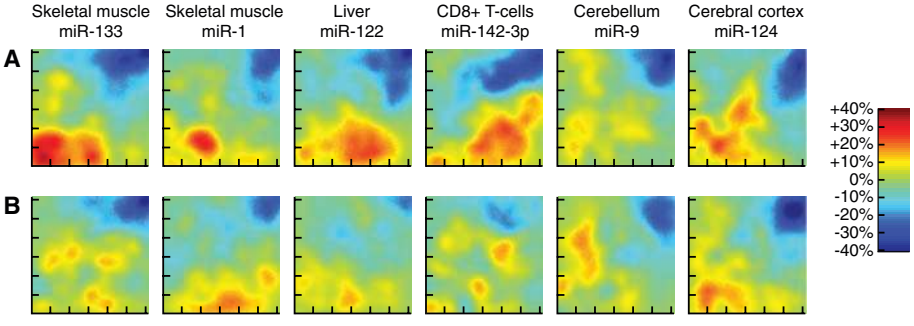

Fig. 3. Density maps for genes with nonconserved sites. (**A**) Messages with site present in mouse 3′UTR but absent in human ortholog. Data are shown as in Fig. 1, but enrichment is relative to matched cohorts (figs. S5 and S6), controlling for UTR length and nucleotide composition. (**B**) Messages with site present in human UTR but absent in orthologous mouse UTR, analyzed as in (A).

of genes that lacked sites in the mouse UTR but contained a site in the human ortholog. Because such messages would not be subject to miRNA-mediated destabilization in mouse, the depletion signal would vanish if it reflected only direct destabilization. However, the signal persisted (Fig. 3B, blue in upper right); mouse genes that were highly and specifically expressed in the tissue were less likely to harbor sites in their human orthologs, indicating that genes preferentially coexpressed with the miRNA have evolved to avoid targeting by that miRNA. The enrichment for genes expressed at low levels also explained some of the many potentially functional nonconserved sites; they accumulate by chance, without consequence, in messages not coexpressed with the miRNA. The reduction in signal in Fig. 3B compared to Fig. 3A hints that species-specific mRNA destabilization might also be frequent, presumably as both neutral and consequential species-specific targeting.

Quantifying selective depletion of sites among messages preferentially expressed in muscle indicated that ~420 of the 8511 genes of the expression atlas are under selective pressure to avoid miR-133 sites. These are "antitargets," an anticipated class of genes not observed previously (*14*). The estimated numbers of antitargets for miR-1, miR-122, miR-142, miR-9, and miR-124 were 300, 190, 170, 240, and 440, respectively—comparable to the numbers of their conserved targets. Extrapolating to include other miRNA families that are also highly expressed with specific spatial or temporal expression patterns, we estimated that selective avoidance of miRNA targeting extends to thousands of genes (SOM text). A signal for messages avoiding targeting in all tissue types would be harder to detect in our analysis. For some messages, acquiring miRNA pairing might be so detrimental that they are under selective pressure to have short UTRs, perhaps helping to explain why highly expressed "housekeeping" genes have substantially shorter UTRs than do other messages (*19*).

In addition to revealing target avoidance, these data extend results of our heterologous reporter system (Fig. 2) into the animal, showing that 7-nt sites are often sufficient to specify a biological effect. Messages expressed highly and specifically in muscle are ~59% less likely than controls to possess a 7-nt match to muscle-specific miR-133 (Fig. 3A). For the other five miRNAs, this depletion averaged 45% (range of 31 to 57%). This extent of depletion implies that as sites for highly expressed miRNAs emerge during sequence drift of UTRs, about half emerge in a context suitable for miRNA targeting—causing either mRNA destabilization or a selective disadvantage sufficient for preferential loss of the site from the gene pool.

Site depletion due to miRNA activity should occur specifically in tissue types expressing the miRNA. To explore the specificity of depletion, we used a modified Kolmogorov-Smirnov (KS) test to determine whether the set of genes with sites in either human or mouse orthologs were expressed at lower levels than cohorts of genes with the same estimated expectation for having sites, controlling for UTR length and nucleotide composition. In muscle, but not in T cells, the set of transcripts with a miR-133 site was depleted compared with those of control cohorts (Fig. 4A). Repeating the miR-133 analysis for all 61 tissues in the mouse atlas showed that this effect was most pronounced in skeletal muscle and heart, the two tissues in which miR-133 is preferentially expressed. Plotting color-coded P values for relative depletion of transcripts with miR-133 sites illustrated a signature reflecting the tissue-specific influence of miR-133 (Fig. 4B, top row).

Signatures for all 73 miRNA families (representing 169 human miRNA genes) conserved among the four sequenced mammals and zebrafish were derived (fig. S7). For many miRNA families that are prominently expressed in specific tissues (*7*–*10*), the signatures corresponded to tissues in which these miRNAs are expressed (Fig. 4B). These included the six families featured in Fig. 3, as well as let-7, miR-99, miR-29, and miR-153 (brain), miR-30 (kidney), miR-194 (liver, gut, and kidney), miR-141 and miR-200b (olfactory epithelium and gut), miR-96 (olfactory epithelium), and miR-375 (pituitary). Eight of these also gave accurate signatures when considering sites in the coding sequences rather than 3′UTRs (SOM text). miR-7 had the highest signal in the pituitary. This miRNA is known to be prefer-

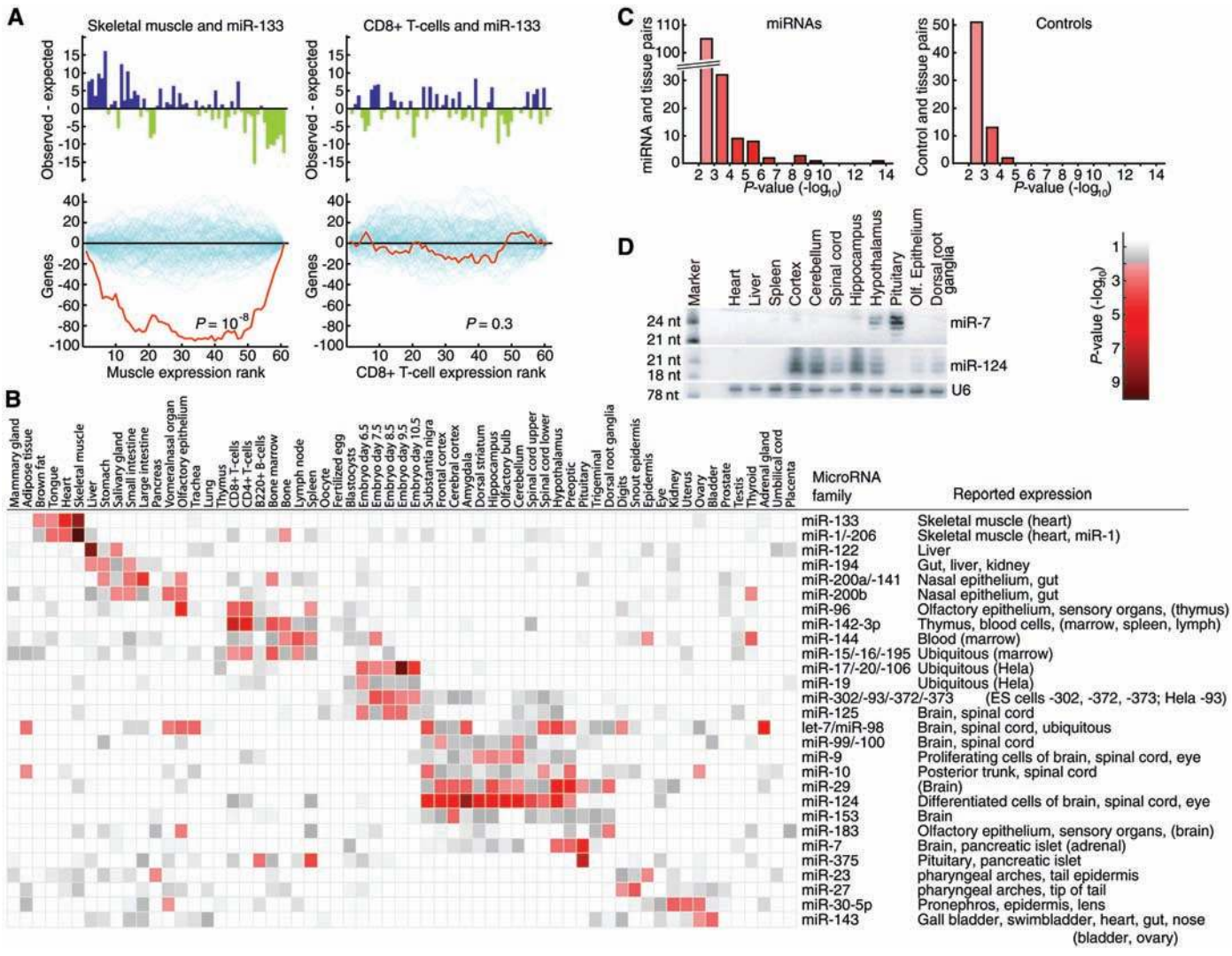

Fig. 4. Depletion of sites in genes preferentially coexpressed with the miRNA. (**A**) miR-133 sites in skeletal muscle and CD8+ T cells. For each panel, genes were binned based on their expression in the indicated tissue compared with expression in the 60 other tissues, with bin 1 lowest and bin 61 highest. (Top) Difference between observed and expected number of messages with miR-133 sites at each expression rank. (Bottom) Modified KS test and estimate of significance, showing the running sum of the difference between the observed and expected distributions across expression ranks for messages with sites (red) compared to control cohorts (blue). (**B**) Summary map of KS tests for each miRNA-tissue pair for 28 miRNAs; *P*-value key is shown above. Reported expression is from zebrafish in situ data (*10*), supplemented with notable mammalian data (*8*, *9*) (parentheses). ES cells, embryonic stem cells. (**C**) Tail of *P*-value distribution for all 73 miRNA families (left) (fig. S7) and for a mock analysis using control sequences (right). *P* values greater than 10^{-2}, which are gray in (B), were only marginally less frequent for controls. (**D**) RNA-blot analysis of miR-7 in rat tissues, reprobed for miR-124 and U6 small nuclear RNA.

entially expressed in the brain (*8*–*10*), but preferential expression in pituitary had not been noted. An RNA blot confirmed that miR-7 expression is highest in the pituitary (Fig. 4D).

Other miRNA families, including most described as having ubiquitous, complex, or undetectable expression patterns, were indistinguishable from controls (Fig. 4C and fig. S7). Nonetheless, some described as ubiquitous displayed stage-specific signatures. These included families in the miR-17~18~19a~20~19b~92 cluster, which had a strong embryo signature, consistent with their association with proliferation and cancer (*20*, *21*). The miR-302 family also had a strong early-embryo signature, consistent with its sequence similarity to the 17~92 proliferation cluster and its expression in embryonic stem cells (*22*, *23*). The conserved targets of these embryonic miRNAs were preferentially at high levels in the oocyte and zygote and then dropped to low levels in the blastocyst and embryo (Fig. 1C), as expected if these miRNAs help dampen expression of maternal transcripts.

A signal for motif conservation is a mainstay of bioinformatics and previously indicated the widespread scope of conserved miRNA targeting (*3*–*5*, *24*), but a signal for absence of a motif is unusual. The ability to observe such a signal revealed an additional dimension to the impact of miRNAs on UTR evolution—a widespread potential for nonconserved targeting leading to the selective loss of many 7-nt sites. When considering conserved targeting, nonconserved targeting, and targeting avoidance, it is hard to escape the conclusion that miRNAs are influencing the expression or evolution of most mammalian mRNAs.

References and Notes

1. D. P. Bartel, *Cell* **116**, 281 (2004).
2. V. Ambros, *Nature* **431**, 350 (2004).
3. B. P. Lewis, C. B. Burge, D. P. Bartel, *Cell* **120**, 15 (2005).
4. J. Brennecke, A. Stark, R. B. Russell, S. M. Cohen, *PLoS Biol.* **3**, e85 (2005).
5. A. Krek *et al.*, *Nat. Genet.* **37**, 495 (2005).
6. A. I. Su *et al.*, *Proc. Natl. Acad. Sci. U.S.A.* **101**, 6062 (2004).
7. M. Lagos-Quintana *et al.*, *Curr. Biol.* **12**, 735 (2002).
8. L. F. Sempere *et al.*, *Genome Biol.* **5**, R13 (2004).
9. S. Baskerville, D. P. Bartel, *RNA* **11**, 241 (2005).
10. E. Wienholds *et al.*, *Science* **309**, 310 (2005).

11. K. K. Tomczak *et al.*, *FASEB J.* **18**, 403 (2004).
12. P. K. Rao, M. Farkhondeh, S. Baskerville, H. F. Lodish, data not shown.
13. M. W. Rhoades *et al.*, *Cell* **110**, 513 (2002).
14. D. P. Bartel, C. Z. Chen, *Nat. Rev. Genet.* **5**, 396 (2004).
15. L. P. Lim *et al.*, *Nature* **433**, 769 (2005).
16. B. P. Lewis, I. H. Shih, M. W. Jones-Rhoades, D. P. Bartel, C. B. Burge, *Cell* **115**, 787 (2003).
17. J. G. Doench, P. A. Sharp, *Genes Dev.* **18**, 504 (2004).
18. E. C. Lai, B. Tam, G. M. Rubin, *Genes Dev.* **19**, 1067 (2005).
19. E. Eisenberg, E. Y. Levanon, *Trends Genet.* **19**, 362 (2003).
20. A. Ota *et al.*, *Cancer Res.* **64**, 3087 (2004).
21. L. He *et al.*, *Nature* **435**, 828 (2005).
22. H. B. Houbaviy, M. F. Murray, P. A. Sharp, *Dev. Cell* **5**, 351 (2003).
23. M. R. Suh *et al.*, *Dev. Biol.* **270**, 488 (2004).
24. X. Xie *et al.*, *Nature* **434**, 338 (2005).
25. We thank G. Ruby, M. Axtell, and H. Chang for helpful discussions. Supported by predoctoral fellowships from the Department of Energy (B.P.L.) and NSF (C.J.) and a postdoctoral fellowship and grants from the NIH (A.G., C.B.B., D.P.B.). D.P.B. is a Howard Hughes Medical Institute Investigator.

Supporting Online Material
www.sciencemag.org/cgi/content/full/1121158/DC1
Materials and Methods
SOM Text
Figs. S1 to S7
Tables S1 and S2
References

11 October 2005; accepted 10 November 2005
Published online 24 November 2005;
10.1126/science.1121158
Include this information when citing this paper.

Ubiquitin-Binding Domains in Y-Family Polymerases Regulate Translesion Synthesis

Marzena Bienko,[1] Catherine M. Green,[2] Nicola Crosetto,[1]* Fabian Rudolf,[3]* Grzegorz Zapart,[1] Barry Coull,[2]† Patricia Kannouche,[2]‡ Gerhard Wider,[4] Matthias Peter,[3] Alan R. Lehmann,[2] Kay Hofmann,[5] Ivan Dikic[1]§

Translesion synthesis (TLS) is the major pathway by which mammalian cells replicate across DNA lesions. Upon DNA damage, ubiquitination of proliferating cell nuclear antigen (PCNA) induces bypass of the lesion by directing the replication machinery into the TLS pathway. Yet, how this modification is recognized and interpreted in the cell remains unclear. Here we describe the identification of two ubiquitin (Ub)–binding domains (UBM and UBZ), which are evolutionarily conserved in all Y-family TLS polymerases (pols). These domains are required for binding of polη and polι to ubiquitin, their accumulation in replication factories, and their interaction with monoubiquitinated PCNA. Moreover, the UBZ domain of polη is essential to efficiently restore a normal response to ultraviolet irradiation in xeroderma pigmentosum variant (XP-V) fibroblasts. Our results indicate that Ub-binding domains of Y-family polymerases play crucial regulatory roles in TLS.

Signaling through ubiquitin (Ub) is generally thought to occur by low-affinity noncovalent interactions between Ub and a variety of specialized Ub-binding domains (UBDs) (*1*, *2*). To analyze the Ub-interaction map, we performed yeast two-hybrid screens using wild-type Ub and Ub in which isoleucine 44 (I44) was mutated to alanine (Ub*). To date, all known characterized UBDs require the conserved I44 in the hydrophobic patch on Ub for their binding (*2*), and proteins interacting with Ub* might therefore contain previously unknown Ub-interacting modules. Among the clones that interacted with Ub* are two that encode the C terminus of TLS polymerase ι (polι) (fig. S1A). Moreover, full-length mouse polι expressed in human embryonic kidney (HEK) 293T cells bound to both glutathione *S*-transferase (GST)–Ub and GST-Ub*, but not to GST alone (fig. S1A). Thus, polι contains a Ub-binding module in the C terminus that does not require I44 for its binding to Ub. Bioinformatic analysis of the C-terminal part of polι identified two copies of a previously unknown sequence motif termed UBM (Ub-binding motif). These repeats span ~30 residues and consist of two predicted helical segments, separated by an invariant "Leu-Pro" motif, which is conserved in all polι versions examined, as well as in Rev1, another Y-polymerase (fig. S1B). Missense mutations of the conserved residues with a presumptive crucial role in Ub binding (L508A, P509A in UBM1*, L693A, P694A in UBM2*) in either polι UBM substantially impaired polι binding to GST-Ub, whereas the inactivation of both domains by point mutations completely blocked the interaction (Fig. 1A). Similar results were obtained using polι UBM deletion (polι-Δ496-524 and polι-Δ681-709) mutants (fig. S1C). We purified isolated GST-UBM1 and GST-UBM2 of polι and analyzed their binding to Ub and the Ub-I44A mutant by nuclear magnetic resonance (NMR) spectroscopy (fig. S1D). The estimated dissociation constant (K_d) values for binding of UBM1 and UBM2 to both Ub and Ub-I44A were in the range of 180 μM. Mapping of the

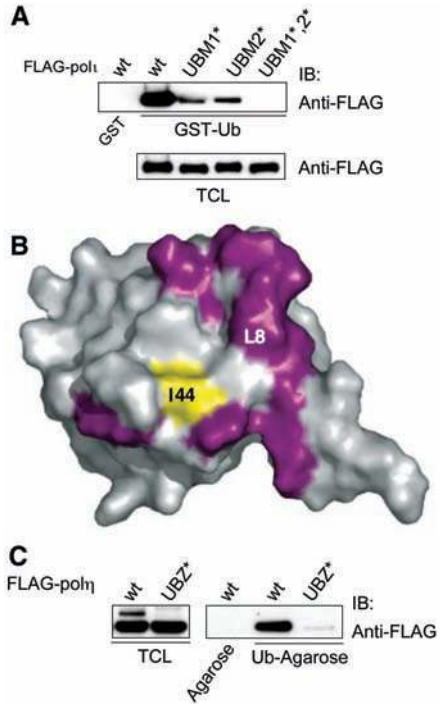

Fig. 1. (**A**) Identification of the UBDs in Y-polymerases. Point mutations of either UBM1 (L508A,P509A in UBM1*) or UBM2 (L693A,P694A in UBM2*) of mouse polι reduce its binding to Ub as compared with wild-type polι (wt). Mutating both UBMs (UBM1*,2*) abolishes binding of polι to Ub in GST pull-down assays. (**B**) Surface representation of Ub interaction with UBM determined by NMR spectroscopy. The binding interface of GST-UBM2 on Ub defined by residues K6, L8, T9, G10, I13, T14, R42, K48, G53, and R72 (see supporting online material) is indicated in purple. Residue I44 (yellow) is indicated for orientation. (**C**) Polη UBZ mediates binding to ubiquitin. HEK293T lysates (TCL) containing FLAG-polη wild type or its UBZ mutant (D652A) (UBZ*) were subjected to Ub-agarose pull-down assays. The shift in mobility of polη visible in lane 1 represents its monoubiquitinated form. IB, immunoblot.

[1]Institute for Biochemistry II, Goethe University Medical School, Theodor-Stern-Kai 7, 60590 Frankfurt, Germany. [2]Genome Damage and Stability, University of Sussex, Falmer, Brighton BN1 9RQ, UK. [3]Institute of Biochemistry, [4]Institute of Molecular Biology and Biophysics, ETH Hönggerberg, 8093 Zürich, Switzerland. [5]Bioinformatics Group, Miltenyi Biotec GmbH, Stoeckheimer Weg 1, D-50829 Koeln, Germany.

*These authors contributed equally to this work.
†Present address: Life Sciences, Unilever R&D, Colworth House, Sharnbrook, Bedford MK44 1LQ, UK.
‡Present address: Laboratory of Genetic Instability and Cancer, CNRS, Institut Gustave Roussy, 94805 Villejuif, France.
§To whom correspondence should be addressed. E-mail: ivan.dikic@biochem2.de